Infrared Phys. Vol. 33, No. 3, pp. 219–226, 1992
Printed in Great Britain.

0020-0891/92 $5.00 + 0.00

EFFECTIVE FAR INFRARED LASER OPERATION WITH MESH COUPLERS

ROLF DENSING,[1] ARNE ERSTLING,[1] MARK GOGOLEWSKI,[1]
HANS-PETER GEMÜND,[2] GUNDULA LUNDERSHAUSEN[2] and ANDREW GATESMAN[3]

[1]Department of Electrical Engineering, University of Virginia, Charlottesville, VA 22903, U.S.A.,
[2]Max-Planck-Institut für Radioastronomie, D-W-5300 Bonn, Fed. Rep. Germany and
[3]Department of Physics and Applied Physics, University of Massachusetts at Lowell, Lowell, MA 01854, U.S.A.

(Received for publication 9 January 1992)

Abstract—In the pursuit of increased far infrared (FIR) laser output power and higher beam quality, we have designed, fabricated and applied hybrid metal mesh couplers. Fourier Transform Spectroscopy was performed to evaluate the spectral characteristics of the couplers. With smallest mesh features of 1.0 μm, these couplers, fabricated in a class 100 clean-room, exhibited remarkably wide bandpass characteristics. Application in an Apollo Model 122 FIR laser system resulted in high output powers on many lines in the 100–500 μm range, with only moderate pump powers (10–60 W). A careful analysis of the FIR laser beam showed undiffracted Gaussian beam profiles with low divergence angles.

INTRODUCTION

For most applications of FIR lasers, sufficient output power on as many lines as possible is equally important as beam quality. To provide optimum coupling to the EH_{11} intracavity mode, thus achieving maximum power and a Gaussian beam profile, hybrid metal mesh couplers[1,2] are preferred over most other coupling techniques, since no aperture diffraction occurs. Mesh dimensions much smaller than FIR wavelengths guarantee an undiffracted laser beam. A low loss substrate is used in order to support the entire coupling structure. A dielectric, infrared (IR) reflection enhanced coating is deposited onto the substrate to provide a $R \geqslant 98\%$ reflectivity for the 10 μm pump radiation, thereby optimizing the pump efficiency. A metal mesh, deposited on top of the IR reflection enhanced coating, determines the FIR properties of the coupler, and provides a uniform reflectivity over its entire surface preserving the intracavity mode. Figure 1 compares the commonly used hole coupler and a hybrid mesh coupler. Interferometric coupling devices[3–8] with a continuously tunable reflectivity are another promising approach to optimize the efficiency of FIR lasers. However, these devices are relatively bulky and introduce even more adjustable elements into the FIR cavity. Also, the positioning of the interferometer elements must be accurately controlled (because of the steep Airy-curve combined with the typically high reflectivity required) to avoid power fluctuations. Application of our mesh-couplers to FIR lasers yields stable output powers of tens of milliwatts on many lines in the 100–500 μm range, even when pumped with moderate powers in the 10–60 W range. Gaussian beam profiles with low divergence angles were achieved in all cases.

DESIGN CONSIDERATIONS

Our coupler design consists of a substrate, an infrared (IR) high-reflection coating, and a metallic mesh (Fig. 2), similar to the original set-up proposed by Danielewicz.[1,2] Monocrystalline silicon and quartz are good choices for substrate materials. N-type silicon (Si) with resistivities $\rho \geqslant 1$ kΩ-cm is reported to have an absorption coefficient $\alpha \leqslant 0.1\ \text{cm}^{-1}$ and a flat dispersion curve.[9] C-cut crystal quartz (ccq) has an absorption coefficient of $\alpha \leqslant 1.2\ \text{cm}^{-1}$ for $\lambda \geqslant 100\ \mu$m.[10] Our investigations with a Fourier Transform Spectrometer qualitatively confirmed these low losses.

Report Documentation Page

Form Approved
OMB No. 0704-0188

1. REPORT DATE	2. REPORT TYPE	3. DATES COVERED
1992		**00-00-1992 to 00-00-1992**

4. TITLE AND SUBTITLE	5a. CONTRACT NUMBER
Effective Far Infrared Laser Operation with Mesh Couplers	5b. GRANT NUMBER
	5c. PROGRAM ELEMENT NUMBER
6. AUTHOR(S)	5d. PROJECT NUMBER
	5e. TASK NUMBER
	5f. WORK UNIT NUMBER
7. PERFORMING ORGANIZATION NAME(S) AND ADDRESS(ES) **University of Massachusetts Lowell,Department of Physics and Applied Physics,Lowell,MA,01854**	8. PERFORMING ORGANIZATION REPORT NUMBER
9. SPONSORING/MONITORING AGENCY NAME(S) AND ADDRESS(ES)	10. SPONSOR/MONITOR'S ACRONYM(S)
	11. SPONSOR/MONITOR'S REPORT NUMBER(S)

12. DISTRIBUTION/AVAILABILITY STATEMENT
Approved for public release; distribution unlimited

13. SUPPLEMENTARY NOTES

14. ABSTRACT

In the pursuit of increased far infrared (FIR) laser output power and higher beam quality, we have designed, fabricated and applied hybrid metal mesh couplers. Fourier Transform Spectroscopy was performed to evaluate the spectral characteristics of the couplers. With smallest mesh features of 1.0 J1. m these couplers, fabricated in a class 100 clean-room, exhibited remarkably wide bandpass characteristics. Application in an Apollo Model 122 FIR laser system resulted in high output powers on many lines in the 100- 500 Jl.m range, with only moderate pump powers (10-60 W). A careful analysis of the FIR laser beam showed undiffracted Gaussian beam profiles with low divergence angles.

15. SUBJECT TERMS

16. SECURITY CLASSIFICATION OF:			17. LIMITATION OF ABSTRACT	18. NUMBER OF PAGES	19a. NAME OF RESPONSIBLE PERSON
a. REPORT	b. ABSTRACT	c. THIS PAGE			
unclassified	**unclassified**	**unclassified**	**Same as Report (SAR)**	**8**	

	HOLE COUPLER	MESH COUPLER
BEAM QUALITY	 HOLE DIAMETER > λ DIFFRACTION DIVERGENT BEAM	 PERIODICITY < λ NO DIFFRACTION
INTRA – CAVITY MODE PROPAGATION	 ▪ SELECTIVE ATTENUATION AT PLACE OF HOLE ▪ EXCITATION OF HIGHER EH_{mn} MODES LIKELY	 ▪ HOMOGENEOUS COUPLING OVER ENTIRE SURFACE ▪ EH_{11} MODE PROPAGATION
PUMP RADIATION	 HOLE REGION LEAKS PUMP RADIATION EXTERNAL ATTENUATOR REQUIRED	 > 98 % REFLECTANCE FOR PUMP RADIATION
ADJUSTMENT OF R, T	CHANGING HOLE DIAMETER AFFECTS SIMULTANEOUSLY IR AND FIR PROPERTIES	CHANGING MESH DESIGN AFFECTS FIR PROPERTIES ONLY

Fig. 1. Comparison of mesh couplers and conventional hole couplers.

Since the coupler is highly exposed to the 10 μm pump radiation, the IR properties of the substrate must be considered. Silicon, with an IR reflection enhanced coating, has a sufficiently high thermal damage threshold to withstand the exposure to high pump power densities.[11] Quartz, however, has a strong absorption band near the 9–10 μm branches of the pump laser,[12] but can withstand some 10 W of CO_2 laser radiation when coated with a highly efficient IR reflection

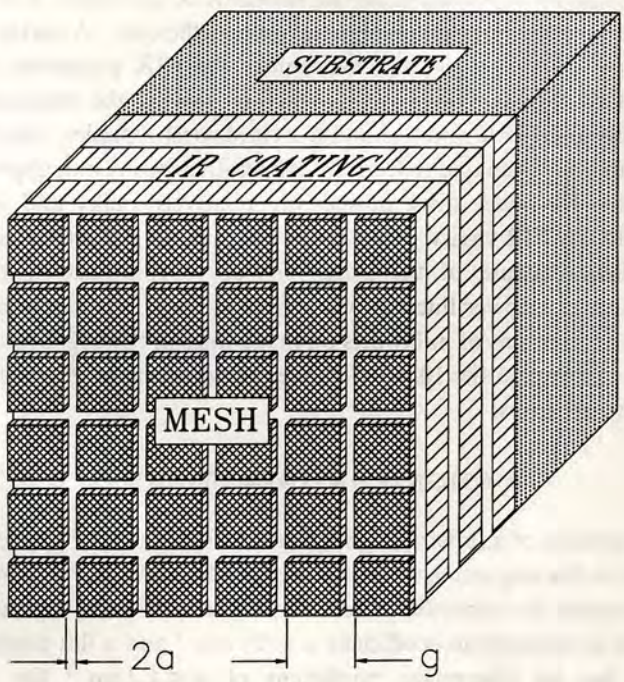

Fig. 2. Schematic of a mesh coupler (not to scale).

coating. A 4- to 5-layer dielectric stack of either Ge and CaF_2, or Ge and ZnS has been shown by means of grating spectrometry to yield a reflectivity which is comparable to the reflectivity of a gold coated optical-quality surface.[13] Since the total (optical) thickness of the coating is much smaller than FIR wavelengths, it is assumed to have only a minor effect on the FIR properties of the coupler.

The FIR properties of a mesh coupler are mainly determined by the mesh dimensions in combination with the refractive index of the substrate (n_{Sub}). The mesh structure is deposited by RF sputtering of gold onto the IR coated substrate, which has been masked with a photoresist pattern, using a standard lithographic process. The thickness (typically several tenths of a micron) of this gold-film should be larger than the skin-depth at the desired wavelength range in order to minimize losses. The mesh usually has the form of either an array of metallic islands (e.g. squares, as in Fig. 2), separated by a gap of width $2a$ (capacitive meshes), or periodic perforations (e.g. squares) in a metallic film, separated by a conducting line of width $2a$ (inductive meshes). Small capacitive meshes are somewhat easier to fabricate and have the additional advantage of covering a larger portion of the surface with gold, which helps to reflect the IR radiation, thereby additionally protecting IR-absorbing substrates from damage.

The useful range of operation for these mesh-structures can be optimized by keeping the ratio of $g/2a$ (g is the periodicity of the mesh) as high as possible, while dimensioning $g \leqslant \lambda_d/n_{eff}$, where n_{eff} is the effective refractive index and λ_d defines the onset of diffraction and should be chosen well below 100 μm. Using the substrates ($n_{Si} \approx 3.42$,[14,15,9] $n_{ccq} \approx 2.1$[10,16]) and coating mentioned above and assuming, that $n_{eff} \approx n_{Sub}$, g is limited to values no higher than 20–40 μm, if we want to avoid diffraction for wavelengths larger than 100 μm. The effect of an increased $g/2a$ ratio on the mesh's bandwidth is demonstrated in Fig. 3, where for simplicity the transmission of a free-standing-inductive mesh is regarded. The solid line represents a measured Fourier Transform Spectrum of a mesh with $g/2a = 3.5$. The dashed line is a relatively close fit, based on an aperture array model.[17–20] Keeping the periodicity of the mesh constant and changing the ratio $g/2a$ to 100 results

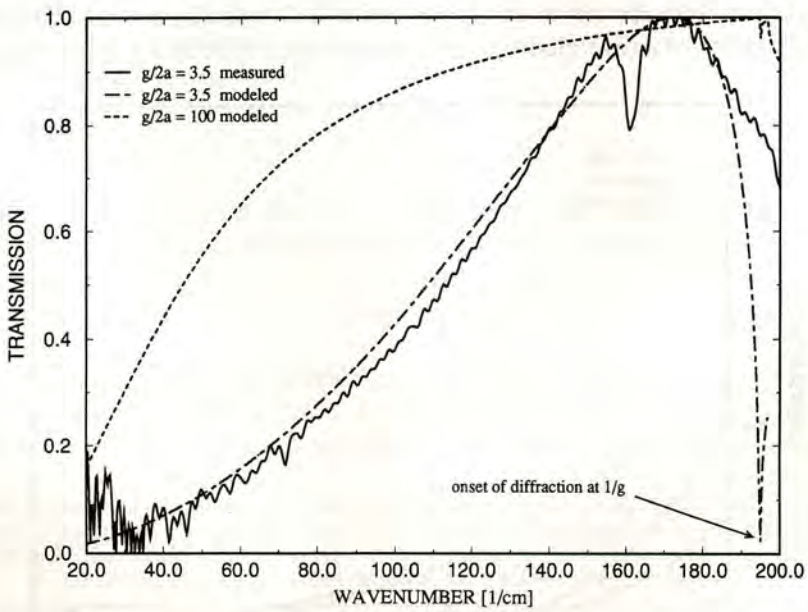

Fig. 3. Spectra of free standing inductive meshes. Solid line: measured spectrum of a mesh with $g = 50.8\ \mu$m, $2a = 14.5\ \mu$m ($g/2a = 3.5$). Dashed line: modeled spectrum of the same mesh. Note the onset of diffraction at $1/g$ ($n = 1$ in Air). The sharp dip at 195 cm^{-1} (in analogy to Wood's anomaly[26,27]) is washed out in the experimental curve, due to a limited resolution of the spectrometer, an imperfect plane incident wave and an imperfect mesh. Dotted line: modeled spectrum of a mesh with $g/2a = 100$.

in a much wider bandpass (dotted line) and a flatter spectral response in the peak region. This behavior can be understood qualitatively by regarding the inductive mesh as an array of apertures and each aperture as a flat waveguide. A higher $g/2a$ ratio is equivalent to a larger waveguide, which transmits a wider frequency range. According to Babinet's theorem,[21] the transmission of an inductive mesh should be equivalent to the reflection of the corresponding capacitive mesh. A wider bandpass and flatter reflection spectrum in the peak region makes it considerably easier, to match a given reflectivity (for a capacitive mesh) to a given wavelength. In addition, an increased $g/2a$ ratio increases the reflection for the 10 μm pump radiation. More details on the properties of metallic meshes are given in the numerous review articles. [22–25]

OPTICAL PROPERTIES

Following these design goals, couplers with different meshes, denoted by their $g/2a$ ratio, were fabricated and tested. The spectral properties of our mesh couplers were evaluated, using a Fourier Transform Spectrometer. By measuring the reflection (R), the transmission (T) and computing the loss (L) from $L = 1 - R - T$ over a bandwidth of at least 100 μm $\leqslant \lambda \leqslant$ 500 μm, the relevant FIR properties of the couplers are fully characterized. Provided that the substrates are not too thick (thickness $\leqslant$ 2 mm), and that the resistivity of the silicon samples is above 900 Ω-cm, the FIR loss of our couplers is less than the uncertainty of the measurement ($\leqslant$ 4%). Figure 4 shows transmission spectra of three different meshes on $\rho = 14$ kΩ-cm silicon substrates, about 1.0 mm thick. The relatively flat spectral response over a wide frequency range makes it particularly easy to predict the reflectivity for a given laser line. Comparing the spectra for the 20/2 and the 40/4 coupler (both have the same $g/2a$ ratio of 10) demonstrates that the spectral response scales very well with the mesh dimensions. This holds only as long as the refractive index of the substrate stays fairly constant, as in the case of silicon. Since square shaped mesh structures were used, the FIR properties are independent of polarization.

EXPERIMENTAL RESULTS

The mesh couplers were applied to an Apollo Model 122 optically pumped FIR laser system. The FIR cavity consists of a (overmoded) dielectric waveguide with an i.d. of 31 mm and a length

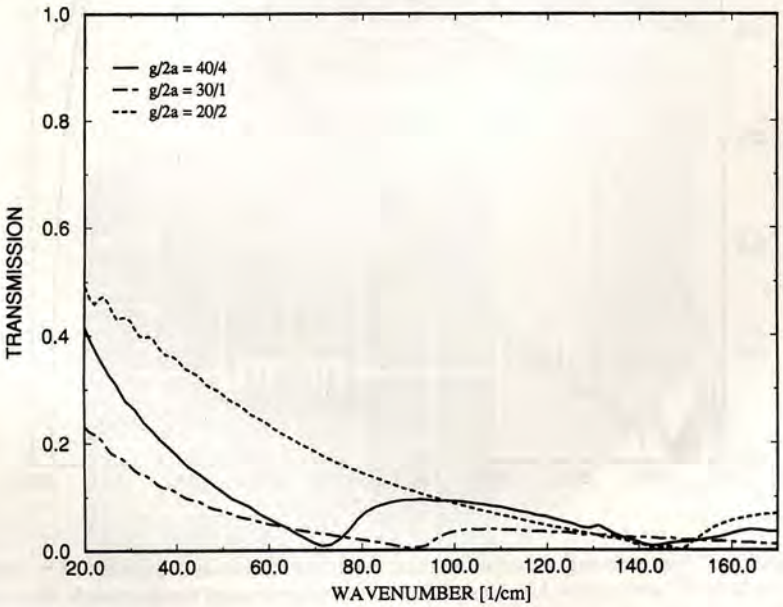

Fig. 4. Measured spectra of 1 mm thick silicon substrates with a $g/2a = 40/4$ (solid line), $g/2a = 30/1$ (dashed line), $g/2a = 20/2$ (dotted line) mesh on it.

Table 1. Selection of FIR laser lines, operated with mesh couplers: Power-data represent direct Scientech 362 readings, frequencies are according to Ref. (29)

Wavelength (μm)	Frequency (GHz)	Laser gas	Pump line	Pump power (W)	Rel. Pol.	QE (%)	FIR power (mW)
119	2522.7816	CH_3OH	9P36	42	$\perp$	5.6	96
158	1891.2742	CH_2F_2	9P10	50	$\parallel$	6.5	92
184	1626.6026	CH_2F_2	9R32	42	$\perp$	21.9	230
191	1562.6559	CH_2F_2	9P22	65	$\parallel$	2.1	33
214	1397.1186	CH_2F_2	9R34	45	$\perp$	4.2	40
393	761.6077	HCOOH	9R18	32	$\parallel$	16.7	63
513	584.3882	HCOOH	9R28	36	$\parallel$	7.7	25

of about 1800 mm. Maximum achieved FIR output powers are listed in Table 1. The power data represent direct Scientech 362 readings[28] and were verified using a second meter of the same type. Both power meters have a 1 in. diameter active area (Peltier cell). The quantum conversion efficiency was calculated according to

$$\mathrm{QE} = 2\frac{P_{\mathrm{FIR}}}{P_{\mathrm{IR}}}\frac{\lambda_{\mathrm{FIR}}}{\lambda_{\mathrm{IR}}},$$

where P_{FIR}, P_{IR}, λ_{FIR} and λ_{IR} are the FIR and IR powers and wavelengths respectively. The factor of 2 arises from the fact that the laser action ceases when the population of the upper and lower energy levels that cause the laser transition become equal.

Applying the mesh couplers to our FIR laser resulted in undiffracted Gaussian beam profiles with extremely low divergence angles. These beam characteristics allow for efficient beam matching in the case that the laser is a part of a sophisticated FIR-optical set up, as e.g. a heterodyne receiver (e.g. Refs 30–32). Our beam analysis was accomplished by scanning a pyroelectric detector element across the laser beam at different positions (z) on the optical axis. The beam radius as a function of distance was determined by using the $1/e^2$ intensity points of the resulting profiles. The origin of the z axis was chosen arbitrarily to be the location of the output coupler, with the positive axis pointed external to the cavity. By applying the propagation laws for the fundamental mode according to Ref. (33) and using a linear regression technique, the beam waist (w_0), and the divergence half angle θ of the beams were computed. The relevant equations, as adopted from Kogelnik and Li 1966,[33] are as follows:

$$w^2(z) = w_0^2 + \left(\frac{\lambda}{\pi w_0}\right)^2 (z - z_0)^2.$$

Applying a linear regression, with the wavelength λ given, and using measured values of $w^2(z)$, yields the best fit for w_0 and z_0. The divergence half angle θ is then determined by:

$$\tan\theta = \frac{\lambda}{\pi w_0}$$

The Gaussian beam parameters, including the regression coefficients R, are given in Table 2 and the fitted $1/e^2$ ray traces are shown in Fig. 5. The data in Table 2 are all taken using the same coupler (based on a ccq substrate). In order not to overload the detector or amplifying networks, the CO_2

Table 2. Laser beam characteristics: all data were taken with the same (ccq-based) coupler. The laser power was attenuated, in order not to overload the detector or amplifying networks. z_0 is measured relative to the laser output coupler. Negative values of z_0 refer to a beam waist, which is located inside the cavity. For positive values the beam waist is located outside the cavity.

Wavelength (μm)	Pump power (W)	FIR power (mW)	z_0 (mm)	w_0 (mm)	R	Divergence angle (deg)
119	18	10	−21	8.9	0.994	0.24
184	16	11	−65	10.1	0.970	0.33
393	21	10	5	8.5	0.998	0.84
513	23	4	12	8.3	0.999	1.13

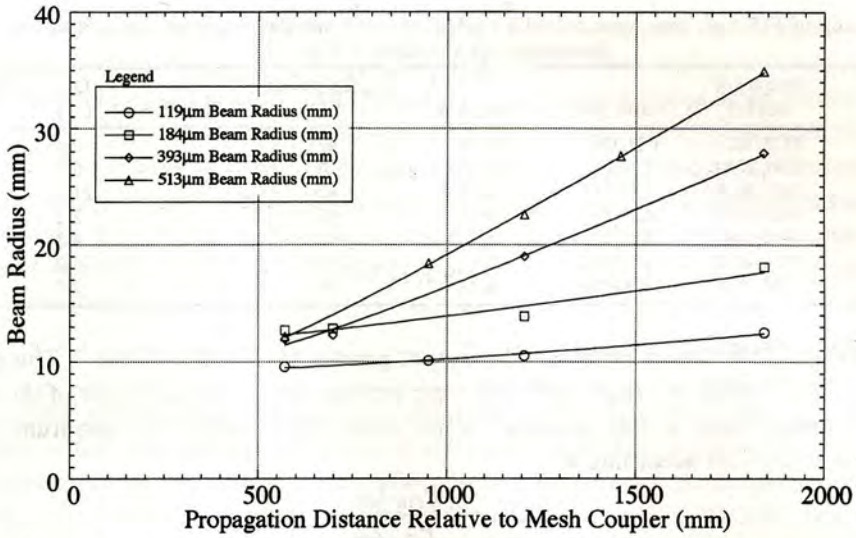

Fig. 5. $1/e^2$ ray traces of mesh coupled laser beams. The error bars are roughly the size of the symbols.

laser pump power was attenuated for this experiment as indicated in the table. Beam profiles for wavelengths between 119 and 513 μm, all taken at the same distance from the mesh coupler, are given in Fig. 6.

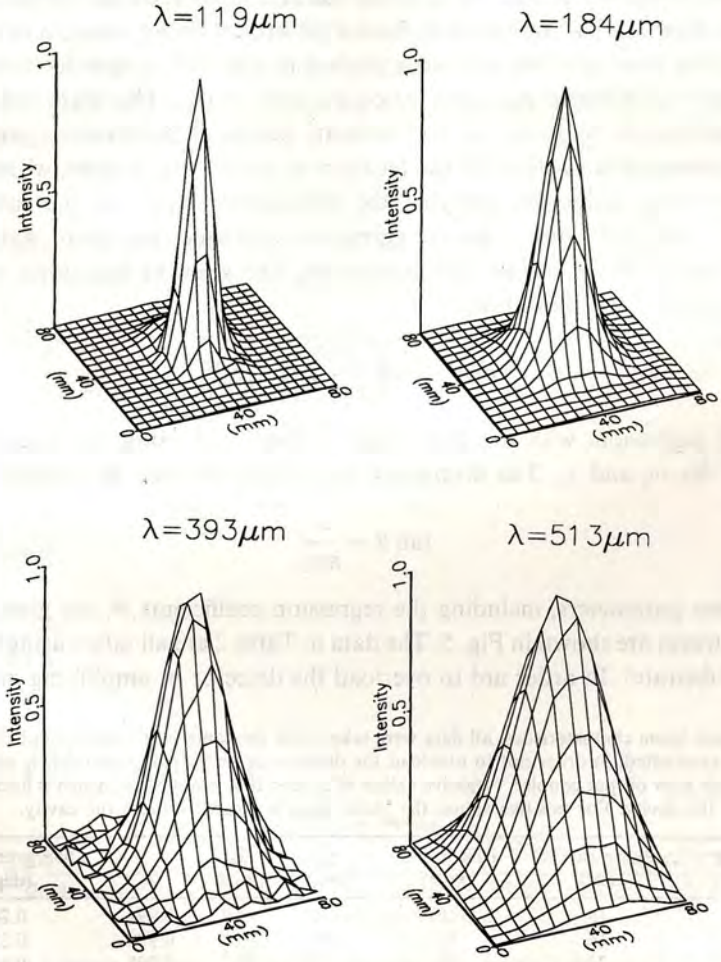

Fig. 6. Typical mesh coupled beam maps. All maps are taken at the same distance from the mesh coupler.

DISCUSSION

Among the many ways to improve the FIR laser power (e.g. increased pump-power, longer FIR cavity or other design changes), the application of mesh couplers seems to be the simplest and most cost effective. A very popular application of FIR lasers is as a local oscillator in a heterodyne receiver. In this application, FIR laser powers in the 1–10 mW range (depending on wavelength) are required to drive the heterodyne mixer in an optimum range.[34] This power requirement can be achieved for many lines using compact CO_2 lasers providing on the order of 15–25 W pump power, as shown in Table 2. In addition, the beam characteristics, demonstrated in Figs 5 and 6, allow for efficient optical coupling. Although our measured beam maps, in combination with a computerized fit method, lead to an accurate determination of the Gaussian beam parameters, the presently available data set is not sufficient to predict any beam parameters without direct measurement. In order to predict the FIR beam parameters as a function of wavelength, the propagation of the pump radiation in the FIR waveguide,[35] and the effect of the input coupler on the pump radiation, need to be considered.

CONCLUSION

FIR laser mesh couplers were designed, fabricated and applied to an Apollo Model 122 laser system. Feature sizes as small as 1.0 μm, fabricated in a class 100 clean room, led to a flat spectral characteristic over a wide frequency range. No measurable absorption loss could be found in the Fourier Transform Spectrometer data. The application of our mesh couplers results in low diverging Gaussian beams and relatively high output powers.

Acknowledgements—The authors gratefully acknowledge Perry Wood and Tim Scholz at the University of Virginia. Perry Wood did the hardware and software development of the beam mapping apparatus and Tim Scholz did most of the coupler application tests. This work was funded in part by the US Army under Contract Number MDA908-86-C-3312.

REFERENCES

1. E. J. Danielewicz, Dissertation, University of Illinois at Urbane-Champaign (1976).
2. E. J. Danielewicz and P. D. Coleman, *Appl. Opt.* **15,** 761 (1976).
3. D. R. Cohn, T. Fuse, K. J. Button, B. Lax, Z. Drozdowicz, *Appl. Phys. Lett.* **17,** 280 (1975).
4. G. Duxbury and H. Herman, *J. Phys. E.: Sci. Instrum.* **11,** 419 (1978).
5. D. T. Hodges, *Infrared Phys.* **18,** 375 (1978).
6. M. S. Tobin, *Digest of the Fourth Int. Conf. IR and Millimeter Waves*, 169 (1979).
7. F. Julien and J-M. Lourtioz, *Int. J. Infrared Millimeter Waves* **1,** 175 (1980).
8. H. P. Röser and R. Wattenbach, *Laser und Optoelektronik* **16,** 165 (1984).
9. D. Grischkowsky, S. Keiding, M. van Exter and Ch. Fattinger, *J. opt. Soc. Am. B* **7,** 2006 (1990).
10. E. V. Loewenstein, D. R. Smith and R. L. Morgan, *Appl. Opt.* **12,** 398 (1973).
11. M. Berger, *ORIEL GmbH Sales Broshure*, "*Eigenschaften optischer Materialien*", Darmstadt, Fed. Rep. Germany (1981).
12. J. B. Heaney, K. P. Stewart and G. Hass, *Appl. Opt.* **22,** 4069 (1983).
13. R. Densing, Dissertation, Universität Bonn (FRG) (1988) (Translated into English by SCITRAN on behalf of NASA GSFC).
14. C. M. Randall and R. D. Rawcliffe, *Appl. Opt.* **6,** 1889 (1967).
15. M. van Exter and D. Grischkowsky, *Appl. Phys. Lett.* **56,** 1694 (1990).
16. K. D. Cummings and D. B. Tanner, *J. opt. Soc. Am.* **70,** 123 (1980).
17. C.-C. Chen, *IEEE Trans. Microwave Theory Tech.* **MTT-18,** 627 (1970).
18. C.-C. Chen, *IEEE Trans. Microwave Theory Tech.* **MTT-19,** 475 (1971).
19. C.-C. Chen, *IEEE Trans. Microwave Theory Tech.* **MTT-21,** 1 (1973).
20. M. S. Durschlag and T. A. De Temple, *Appl. Opt.* **20,** 1245 (1981).
21. A. Babinet, *Compt. Rend.* **4,** 638 (1837).
22. K. F. Renk and L. Genzel, *Appl. Opt.* **1,** 643 (1962).
23. P. Vogel and L. Genzel, *Infrared Phys.* **4,** 257 (1964).
24. R. Ulrich, *Infrared Phys.* **7,** 37 (1967).
25. K. Sakai and L. Genzel, *Rev. Infrared Millimeter Waves* **1,** 155 (1983).
26. R. W. Wood, *Phil. Mag.* **4,** 396 (1902).

27. R. C. Mc Pheadran and D. Maystre, *Appl. Phys.* **14,** 1 (1977).
28. F. B. Foot, D. T. Hodges and H. B. Dyson, *Int. J. Infrared Millimeter Waves* **2,** 773 (1981).
29. M. Inguscio, G. Moruzzi, K. M. Evenson and D. A. Jennings, *J. appl. Phys.* **60,** R161 (1985).
30. H.-P. Röser, *Infrared Phys.* **32,** 385 (1991).
31. R. Titz, B. Auel, W. Esch, H. P. Röser and G. Schwaab, *Infrared Phys.* **30,** 435 (1990).
32. F. Schäfer and P. B. van de Wal, *Proc. of the European Quasi Optical Workshop*, Bonn, Fed. Rep. Germany (1987).
33. H. Kogenik and T. Li, *Proc. IEEE* **54,** 1312 (1966).
34. R. Titz, H.-P. Röser, G. W. Schwaab, P. A. Wood, H. J. Nielson, T. W. Crowe, W. C. Peatman, J. Prince, B. S. Deaver, H. Alius and G. Dodel, *Int. J. Infrared Millimeter Waves* **11,** 809 (1990).
35. A. Harth, *Int. J. Infrared Millimeter Waves* **12,** 221 (1991).